[4] a) G. T. Rado, "Theory of the microwave permeability tensor and Faraday effect in nonsaturated ferromagnetic materials," *Phys. Rev.*, vol. 89, p. 529, 1953.
b) ——, "On the electromagnetic characterization of ferromagnetic media: Permeability tensors and spin wave equations," *IRE Trans. Antennas Propagat.* (*Proc. Symp. Electromagnetic Wave Theory*), vol. AP-4, pp. 512–525, July 1956.
[5] J. J. Green, E. Schloemann, F. Sandy, and J. Saunders, "Characterization of the microwave tensor permeability of partially magnetized materials," Semiannual Rep. RADC-TR-69-73, Feb. 1969.
[6] E. Schloemann, "Microwave behavior of partially magnetized ferrites," *J. Appl. Phys.*, vol. 41, p. 204, 1970.
[7] D. Polder and J. Smit, "Resonance phenomena in ferrites," *Rev. Mod. Phys.*, vol. 25, p. 89, 1953.
[8] R. I. Joseph and E. Schloemann, "Transient and steady state absorption of microwave power under parallel pumping theory," *J. Appl. Phys.*, vol. 38, p. 1915, 1967.

A Catalog of Low Power Loss Parameters and High Power Thresholds for Partially Magnetized Ferrites

JEROME J. GREEN, SENIOR MEMBER, IEEE, AND FRANK SANDY

(Invited Paper)

***Abstract*—The low power loss and high power threshold properties have been measured on a number of candidate ferrite phase-shifting materials. The low power loss is characterized by μ_0'', the imaginary part of the diagonal component of the permeability tensor for the completely demagnetized state. μ_0'' was measured from 3.0 to 16.8 GHz.**

The high power properties are characterized by the parallel pump threshold at a bias field corresponding to $H_i \cong 0$ and to $4\pi M \cong 4\pi M_s$. The threshold was measured between 3.0 and 16.8 GHz. For the purposes of computer calculation μ_0'' and h_{crit} were fit to an equation of the form $A(\gamma 4\pi M_s/\omega)^N$. Translating μ_0'' and h_{crit} to ΔH_{eff} and ΔH_k gives the YIG plus Al as the lowest loss and lowest threshold materials followed by the Gd garnets and MgMn spinels. The Ni spinels are very lossy.

I. INTRODUCTION

In a previous paper [9], it was shown that the microwave properties of partially magnetized materials could be characterized by a permeability tensor similar to that for a fully magnetized material. The real parts of the tensor components were shown to be dependent upon the normalized average magnetization $\gamma 4\pi M/\omega$, the normalized saturation magnetization $\gamma 4\pi M_s/\omega$, and were more or less independent of composition. It was also shown that if $\gamma 4\pi M_s/\omega \leq 0.75$, the loss as determined by the imaginary parts of these components could be characterized by a single parameter μ_0'' the value of μ'' for the completely demagnetized state. Thus the loss characterization is independent of $\gamma 4\pi M/\omega$ but does depend upon $\gamma 4\pi M_s/\omega$ and composition. In order to utilize materials in a given compositional family over a wide class of applications it is necessary to know how μ_0'' for each composition varies with $\gamma 4\pi M_s/\omega$. Therefore, we measured μ_0'' on a number of candidate phase shifter materials as a function of frequency between 3 and 16.8 GHz.

Manuscript received September 22, 1973; revised December 14, 1973. This work was supported in part by the U. S. Air Force Systems Command, Rome Air Development Center, under Contract F30602-68-C-0005.

The authors are with the Research Division, Raytheon Company, Waltham, Mass. 02154.

In addition to requiring knowledge of a phase shifter's low power insertion loss, it is also desirable to anticipate the peak power limitation of the device. Therefore, for the purposes of establishing peak power ratings we have also measured the parallel pump threshold of these candidate phase-shifter materials.

In actual device usage the increase of insertion loss at elevated power levels can occur either by parallel or transverse pumping. Studies have been made by Patton and Green [1]–[3] of the effect upon threshold of sample geometry and of the orientation of the RF magnetic field with respect to the dc magnetization. While these studies show that there is a geometry and orientation dependence, for the purposes of comparing materials the parallel pump threshold at the demagnetization point (i.e., $H_i \cong 0$, $4\pi M \cong 4\pi M_s$, $H_{\text{dc}} = N_z 4\pi M_s$) has been chosen. The measurements are made on spheres because it is easy to obtain spherical samples, it is an easy geometry to measure, and one can easily maintain uniform dc and RF fields inside the sample. The choice of parallel pumping and the choice of the bias points $H_{\text{dc}} = 4\pi M_s/3$ (i.e., $N_z = 1/3$ for a sphere) are motivated by the fact that through the partially magnetized region this bias point and this dc–RF orientation have the lowest threshold. In most device geometries both transverse and parallel orientation conditions exist so that it is probably a parallel pump effect which causes the first increase of insertion loss at elevated power levels.

II. EXPERIMENTAL PROCEDURE

Measurements of μ'' in the demagnetized state were made on thick slabs placed on the end wall of TE_{102} rectangular transmission cavities. The values of μ_0'' (along with μ_0') were calculated from the change in frequency and Q of the cavity between high and low field using an exact solution for the fields in a heavily loaded cavity. A theoretical calculation was also used to correct for the change in copper loss in going from the high field cavity frequency to the low field cavity frequency. Further details can be found in [4].

The technique for determining threshold field is described in [1]. The automatic technique was used for the measurements at 5.5, 9.15, and 16.5 GHz but not in the 3.0-GHz measurements. The more common point by point technique was employed at 3.0 GHz.

III. MICROWAVE LOSS

The loss parameter μ_0'' has been measured on materials made at Raytheon, Trans Tech, and Airtron. μ_0'' is plotted versus $\gamma 4\pi M_s/\omega$ in Figs. 1–4 for the following four classes of materials.

1) Yttrium iron garnets with aluminum and/or gadolinium substitutions, made by Trans Tech.

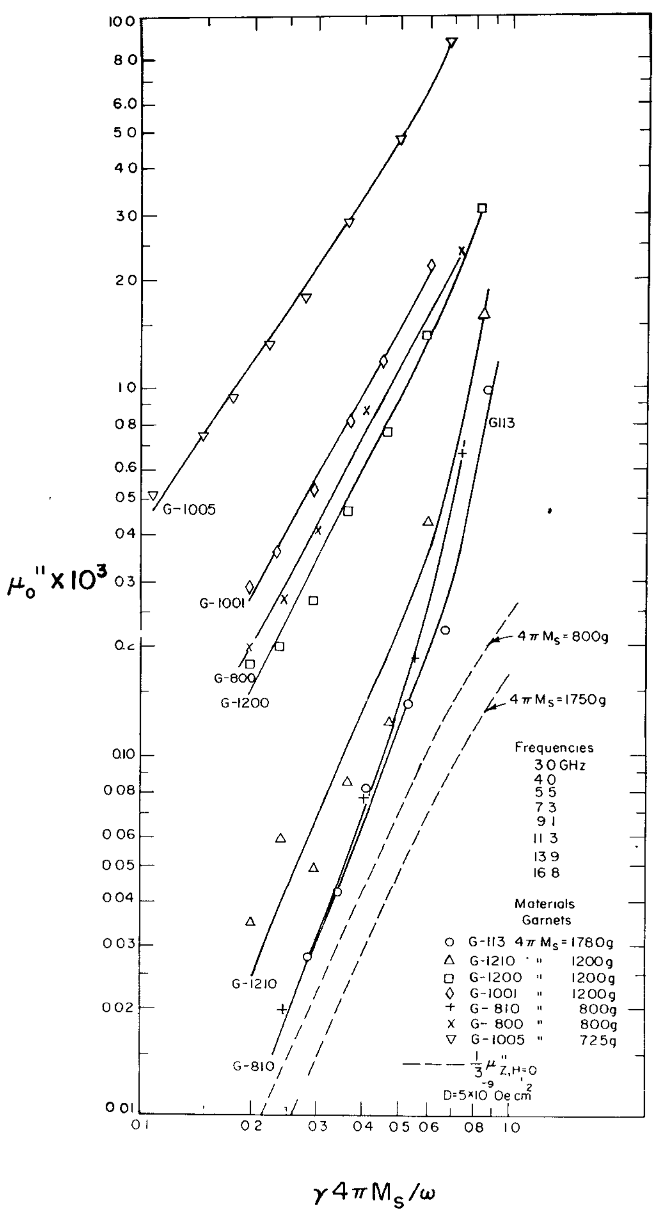

Fig. 1. μ_0'' versus $\gamma 4\pi M_s/\omega$ for various Trans Tech garnets.

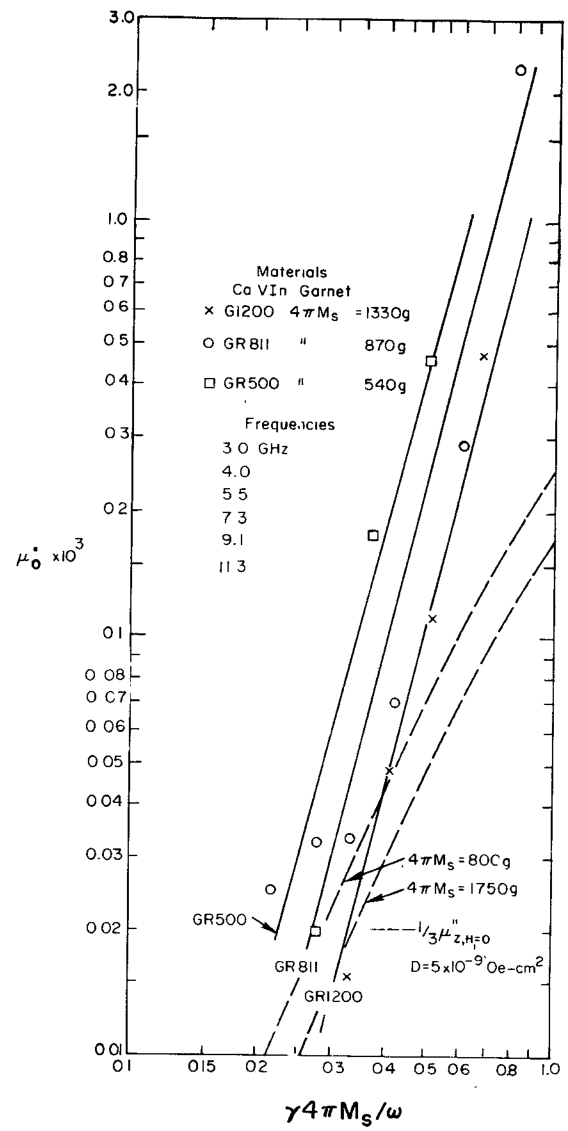

Fig. 2. μ_0'' versus $\gamma 4\pi M_s/\omega$ for various Raytheon CaV in garnets.

2) Yttrium calcium vanadium indium garnets made by Raytheon.

3) Magnesium manganese ferrites with aluminum substitution to reduce $4\pi M_s$ or zinc substitution to increase $4\pi M_s$, made by Trans Tech, Airtron, and Raytheon.

4) Nickel ferrites with aluminum and cobalt substitution made by Trans Tech.

For values of $\gamma 4\pi M_s \omega < 0.7$ the data for almost all of the materials follow a simple power law relationship:

$$\mu_0'' = A \left(\frac{\gamma 4\pi M_s}{\omega}\right)^N \quad (1)$$

where A and N are tabulated in Table I. At larger values of $\gamma 4\pi M_s/\omega$, μ_0'' turns up sharply as Polder–Smit [5] losses set in.

Because μ_0'' is very sensitive to $\gamma 4\pi M_s/\omega$ it is frequently more illuminating to describe materials by an effective linewidth ΔH_{eff} [6]. This effective linewidth is proportional to the damping parameters which appear in either the Landau–Liftshitz or Gilbert torque equations. If one

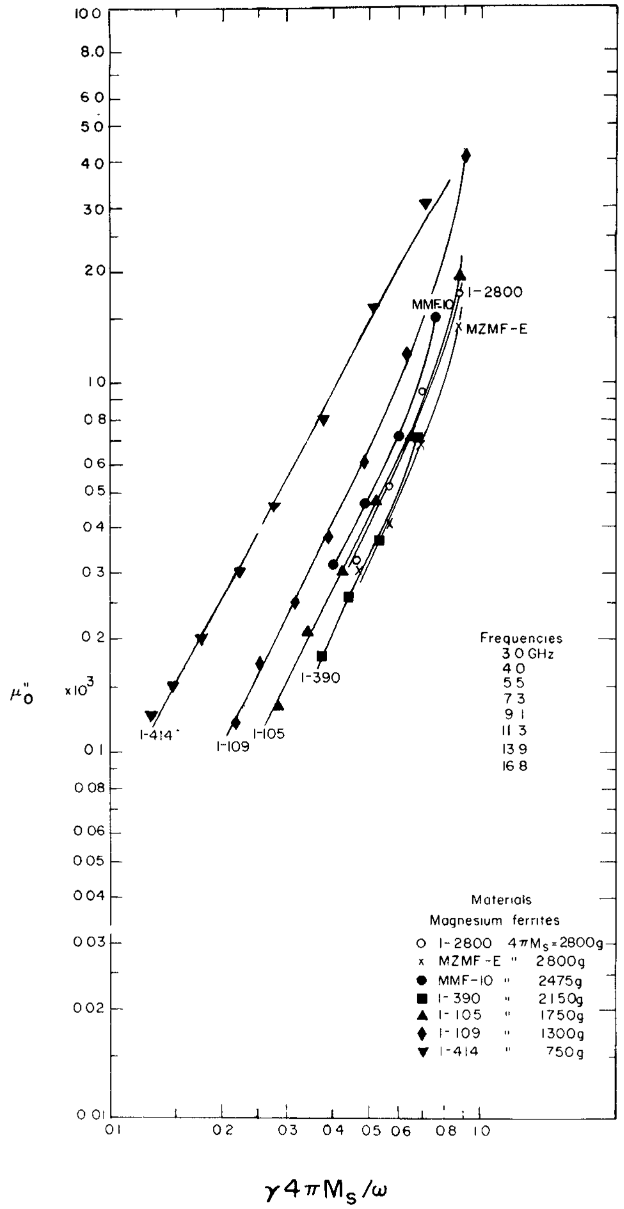

Fig. 3. μ_0'' versus $\gamma 4\pi M_s/\omega$ for magnesium ferrites.

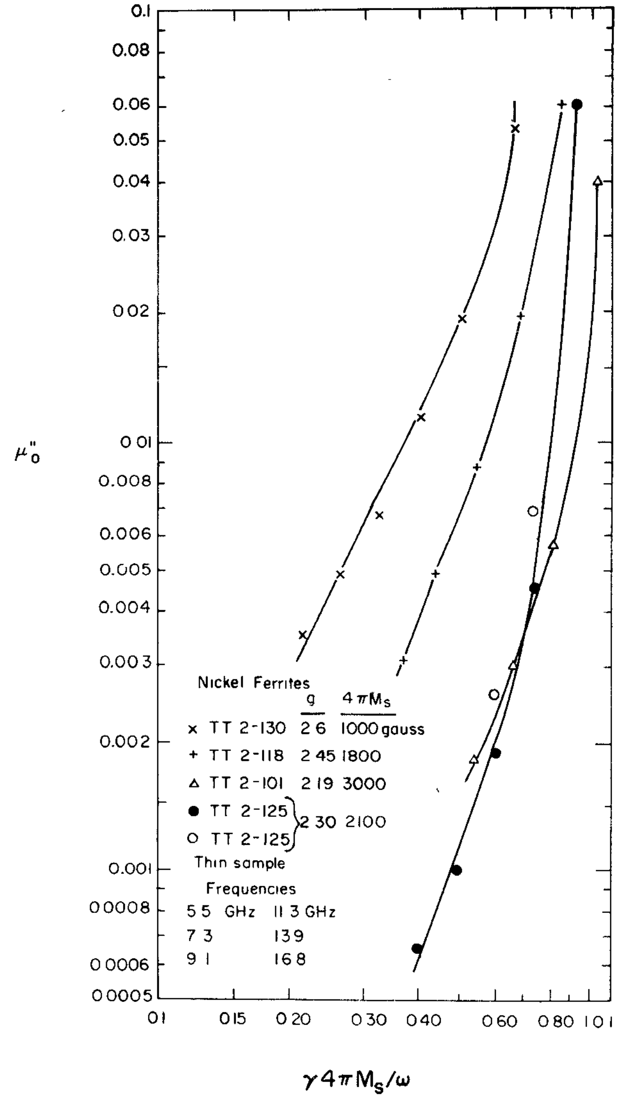

Fig. 4. μ_0'' versus $\gamma 4\pi M_s/\omega$ for nickel ferrites.

solves the torque equations for the permeability of a fully magnetized sample and lets the internal biasing field H_i approach zero one obtains

$$\mu_{H_i=0}'' = \frac{\gamma \Delta H_{\text{eff}}}{2} \frac{\gamma 4\pi M_s}{\omega^2}. \tag{2}$$

Equation (2) illustrates why μ'' varies strongly with ω.

In the demagnetized state, the value of μ'' is the average of the losses over all the randomly oriented domains. On the average any given domain will have two-thirds of its magnetization perpendicular to the RF drive field and one-third of its magnetization parallel to the RF field. If $\omega \gg \gamma 4\pi M_s$, the perpendicular component of the magnetization will produce a contribution to the microwave loss equal to that of a perpendicularly pumped saturated sample at zero internal field, $\mu_{H_i=0}''$, given by (2). In a polycrystalline material ΔH_{eff} can be considerably less than the ferromagnetic resonance linewidth. The component of the magnetization parallel to the RF field makes a contribution to the loss equal to that of a parallel-pumped saturated sample at zero internal field. Joseph and Schlömann [7] have shown that this loss, $\mu_{z,H_i=0}''$, is the result of subthreshold parallel pumping of spin waves. Its magnitude depends on $\gamma 4\pi M_s/\omega$, temperature, and the exchange constant, but not on any material loss mechanisms. It has been calculated using the exchange constant of YIG ($D = 5 \times 10^{-9}$ Oe·cm^2) and $4\pi M_s$ of 1750 and 800 G, and is plotted in Figs. 1 and 2 to show its approximate magnitude. This contribution to the loss is only significant for the low loss garnets so that the use of the exchange constant of YIG is not an unreasonable assumption.

Thus we may represent μ_0'' as

$$\mu_0'' = \tfrac{2}{3}\mu_{H_i=0}'' + \tfrac{1}{3}\mu_{z,H_i=0}'' \tag{3}$$

where $\gamma 4\pi M_s/\omega \ll 1$. From (1) and (3) we can calculate ΔH_{eff}:

TABLE I

Material	Source[a]	Composition	$4\pi M_s$ (gauss)	A	N	ΔH_{eff} at $\gamma 4\pi M_s/\omega = 0.5$ (Oe)	$k \to 0$: B (Oe)	$k \to 0$: ℓ	$k \to 0$: ΔH_k at $\gamma 4\pi M_s/\omega = 0.5$ (Oe)	$H_{dc} = \frac{4\pi M_s}{3}$: B (Oe)	$H_{dc} = \frac{4\pi M_s}{3}$: ℓ	$H_{dc} = \frac{4\pi M_s}{3}$: ΔH_k at $\gamma 4\pi M_s/\omega = 0.5$ (Oe)
G-113	TT	YIG	1780	7.5×10^{-4}	2.5	2.	2.3	.69	1.9	3.2	1.1	3.5
G-1210	TT	YIG + Al	1200	10	2.4	2.	3.0	1.0	3.0	3.5	1.5	4.8
G-1200	TT	YIG + Al + Gd	1200	34	1.9	12.	5.0	1.4	6.7	6.6	1.5	9.2
G-1001	TT	YIG + Gd	1200	50	1.8	20.	6.6	1.4	8.8	8.4	1.5	11.7
G-810	TT	YIG + Al	800	7.6	2.8	.5	.85	1.3	1.0	1.1	1.6	1.6
G-800	TT	YIG + Al + Gd	800	43	1.9	10.	4.5	1.4	6.1	5.6	1.6	8.2
G-1005	TT	YIG + Gd	725	130	1.5	39.	6.8	1.6	10.7	11.9	1.6	17.7
1-2800	TT	MgMnZn ferrite	2800	20	2.2	14.	6.2	.74	5.2	6.8	1.4	8.8
MzMF-E	Ray	MgMnZn ferrite	2800	16	2.2	11.	8.5	.75	7.2	9.3	1.4	12.3
MMF-10	A	MgMn ferrite	2475	20	2.0	14.	4.2	1.1	4.4	4.1	1.6	6.3
1-390	TT	MgMn ferrite with second phase	2150	16	2.2	8.	3.6	1.1	3.8	3.3	1.6	5.0
1-105	TT	MgMn ferrite + Al	1750	18	2.0	9.	3.8	1.3	4.7	4.7	1.6	7.2
1-109	TT	MgMn ferrite + Al	1300	28	1.9	11.	2.7	1.7	4.3	4.8	1.7	7.6
1-414	TT	MgMn ferrite + Al	750	52	1.8	13.	2.4	2.3	5.8	6.4	1.5	8.9
2-101	TT	NiCo ferrite $g = 2.19$	3000	100	2.9	48.	27.0	.95	26.0	26.3	1.4	34.6
2-125	TT	NiAl ferrite $g = 2.30$	2100	95	3.0	30.	11.8	.98	23.2	10.9	1.4	13.9
2-118	TT	NiAlCo ferrite $g = 2.45$	1800	470	2.9	140.						
2-130	TT	NiAl ferrite $g = 2.60$	1000	800	2.1	220.						
GR 1200	Ray	YCaVIn Garnet	1330	18	4.0	1.	1.8	.99	1.8	2.3	1.4	3.1
GR 811	Ray	YCaVIn Garnet	870	40	4.0	2.	2.6	.87	2.4	2.1	1.6	3.1
GR 500	Ray	YCaVIn Garnet	540	60	4.0	2.	1.8	.91	1.7	1.7	1.4	2.2

[a] Manufacturers: TT–Trans Tech; Ray–Raytheon; A–Airtron.

$$\Delta H_{\text{eff}} = 4\pi M_s \left(\frac{\gamma 4\pi M_s}{\omega}\right)^{-2} [3\mu_0'' - \mu_{z,H_i=0}''] \tag{4}$$

$$= 4\pi M_s \left(\frac{\gamma 4\pi M_s}{\omega}\right)^{-2} \left[3A \left(\frac{\gamma 4\pi M_s}{\omega}\right)^{N} - \mu_{z,H_i=0}''\right]. \tag{5}$$

For all but the very lowest loss materials, the subthreshold parallel pump loss can be neglected so that the measured constant A gives the magnitude of ΔH_{eff} and $2 - N$ gives its frequency dependence. This dependence can be positive or negative depending on the loss mechanism involved. The values of ΔH_{eff} obtained from (5) evaluated at $\gamma 4\pi M_s/\omega = 0.5$ are also listed in Table I for comparison with ΔH_{eff} values obtained by other sources.

In addition to the quantitative results shown in Figs. 1–4 and Table I, the following qualitative features are worth noting.

1) Trans Tech Garnets with Aluminum and/or Gadolinium Substitution: Aluminum substitution reduces $4\pi M_s$ without significantly changing the loss parameter A. Gadolinium substitution, on the other hand, substantially increases the loss parameter A and gives ΔH_{eff} a positive frequency dependence which increases with Gd content. The pure and the Al substituted YIG have a negative frequency dependence for ΔH_{eff}.

2) Raytheon's YCaVIn Garnets: These garnets have low loss, comparable to pure YIG and approaching that due to the subthreshold parallel pump loss alone at low $\gamma 4\pi M_s/\omega$ values. Since the Curie temperature of YCaVIn garnets is slightly less than that of YIG, a slightly lower exchange constant than that of YIG should be used in the calculation of the subthreshold parallel pump loss. This would result in a slightly lower subthreshold parallel pump loss and the apparent crossing of the curves in Fig. 2 at low values of $\gamma 4\pi M_s/\omega$ would not occur. The frequency dependence of ΔH_{eff} given by $(2 - N)$ is negative and relatively large. This μ_0'' drops extremely rapidly as $4\pi M_s/\omega$ drops below 1.0.

3) Magnesium Manganese Ferrites: Aluminum substitution lowers $4\pi M_s$, and increases the loss parameter A. The frequency dependence of ΔH_{eff} is almost zero with no aluminum and becomes increasingly positive with more aluminum. Zinc substitution increases $4\pi M_s$ with little change on the loss parameters.

4) Nickel Ferrites: Both aluminum and cobalt substitution increase the loss in this system. The lowest loss member of this group is TT2-125, containing only aluminum, followed very closely by TT2-118 with both aluminum and cobalt. The frequency dependence of ΔH_{eff} is negative for all members except TT2-130, the lossiest sample, for which it is nearly zero.

An additional phenomenon peculiar to this series is that the upturn in μ_0'' as $\gamma 4\pi M_s/\omega$ approaches 1.0 occurs at substantially different values of ω_M/ω for each member of the series. For TT2-101 the break does not occur until $\gamma 4\pi M_s/\omega \approx 0.9$, while for TT2-130, it is as low as 0.6.

Due to their high loss, some of the nickel ferrite samples as originally cut were too thick to measure accurately. All of them were thinned, reannealed, and remeasured. Thus two sets of data were available on some of the samples. The results were usually the same; however, in one case (the X-band measurements on TT2-125), the thinned samples showed 50 percent more loss. The cause for the change was not further explored, but the possibility that some of the samples are inhomogeneous cannot be ignored.

IV. HIGH POWER THRESHOLD

Parallel pump thresholds were measured on the same set of materials, with the exception of TT2-130 and TT2-118, for which μ_0'' was measured. The thresholds were determined at two dc fields, $H_{dc} = 4\pi M_s/3$ and $H_{dc} = H_{k\to 0}$. The threshold at $H_{dc} = 4\pi M_s/3$ is most closely related to a device threshold while that for the low k spin waves, $h_{crit}(k \to 0)$, is given to enable one to compare these thresholds to those of other sources [8]. The measurements were made at 3.0, 5.5, 9.2, and 16.8 GHz and the results are given in Figs. 5–13.

The parallel pump threshold is related to the spin wave linewidth by the relation

$$h_{crit} = \frac{\omega}{\gamma 4\pi M_s} \Delta H_k. \tag{6}$$

If ΔH_k does not depend on frequency then, as seen in Figs. 5–13, h_{crit} can be expected to increase with frequency. The data in these figures have been fit by a series of straight lines which obey a relation similar to (1) for μ_0'':

$$h_{crit} = B\left(\frac{\omega}{\gamma 4\pi M_s}\right)^l. \tag{7}$$

From this and (6) it follows that

$$\Delta H_k = B\left(\frac{\omega}{\gamma 4\pi M_s}\right)^{l-1}. \tag{8}$$

Values of B and l are given in Table I for the two bias conditions, $k \to 0$ and $H_{dc} = 4\pi M_s/3$. Using these values

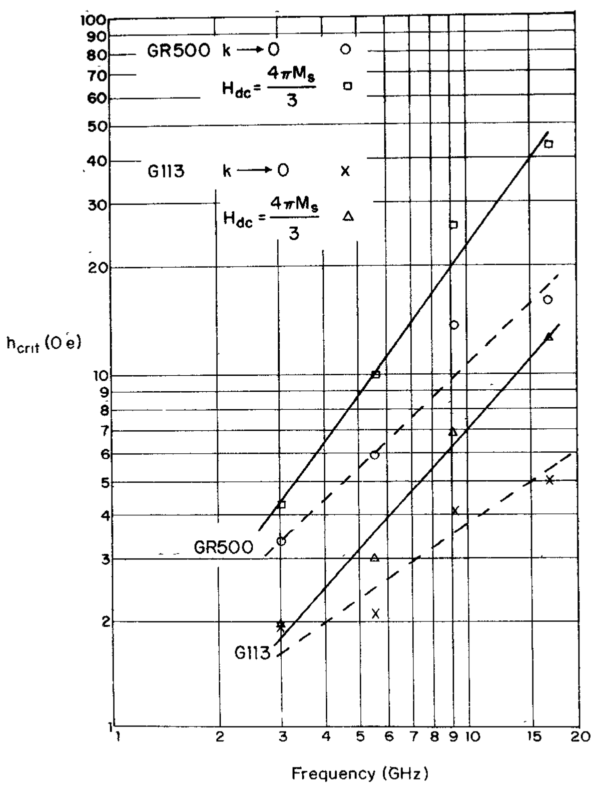

Fig. 5. h_{crit} versus frequency for GR500 and G113.

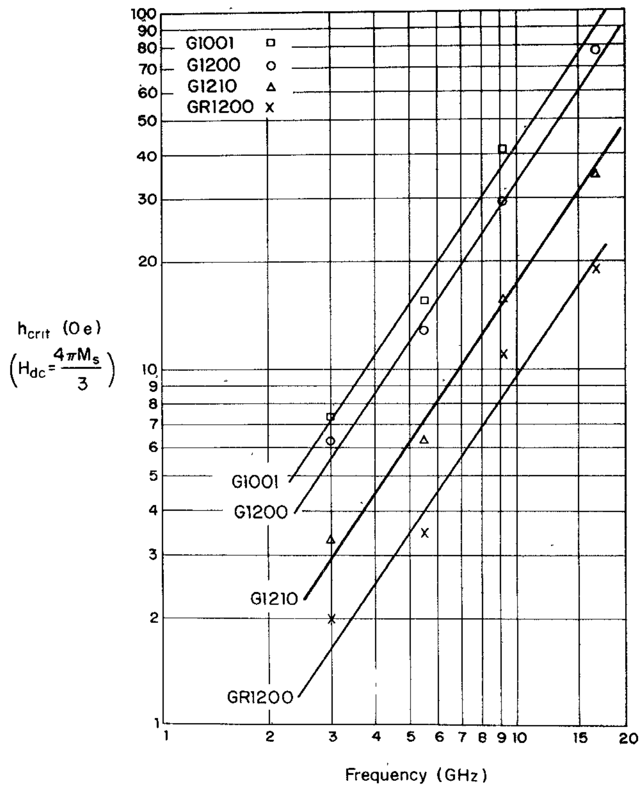

Fig. 6. $h_{crit}(H_{dc} = 4\pi M_s/3)$ versus frequency for G1001, G1200, G1210, and GR1200.

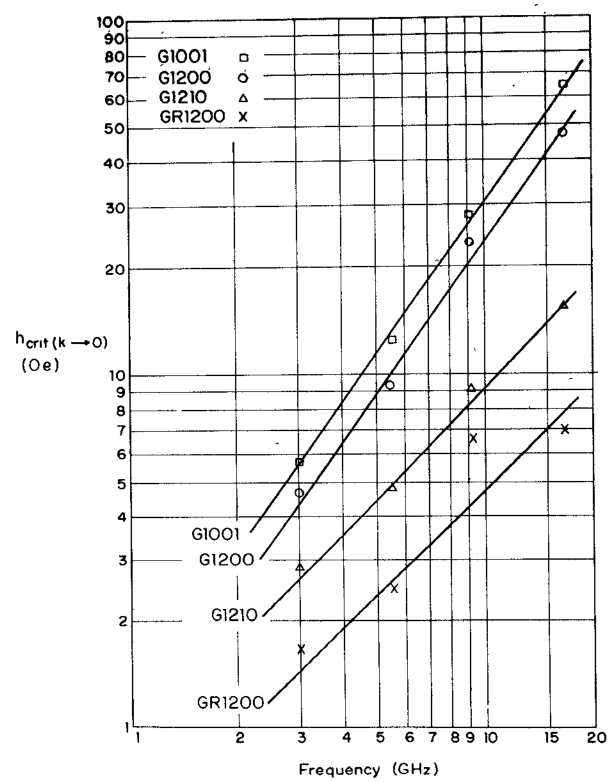

Fig. 7. $h_{crit}(k \to 0)$ versus frequency for G1001, G1200, G1210, and GR1200.

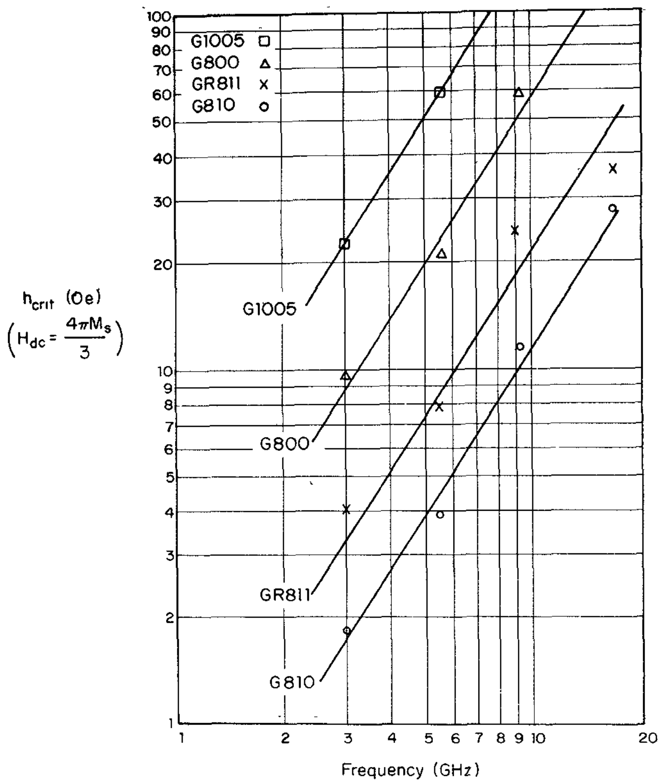

Fig. 8. $h_{crit}(H_{dc} = 4\pi M_s/3)$ versus frequency for G1005, G800, GR811, and G810.

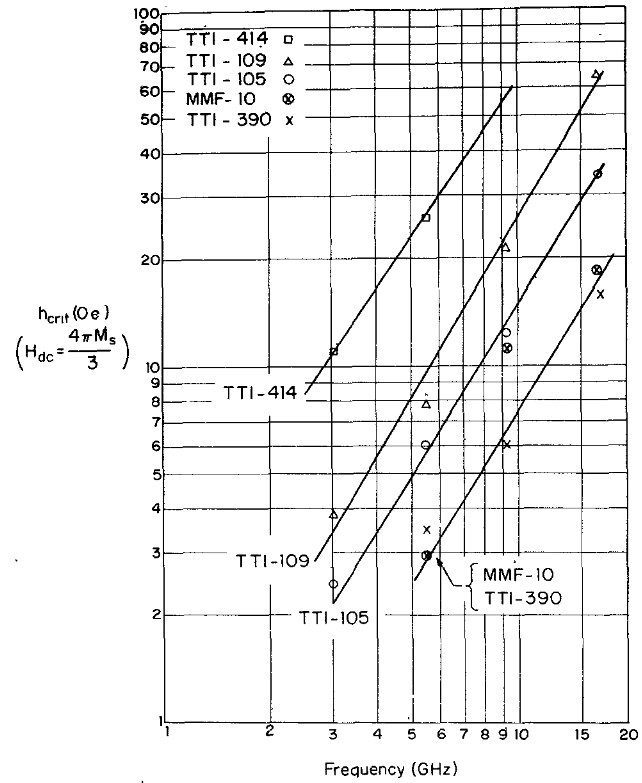

Fig. 10. $h_{crit}(H_{dc} = 4\pi M_s/3)$ versus frequency for TT1-414, TT1-109, TT1-105, MMF-1, and TT1-390.

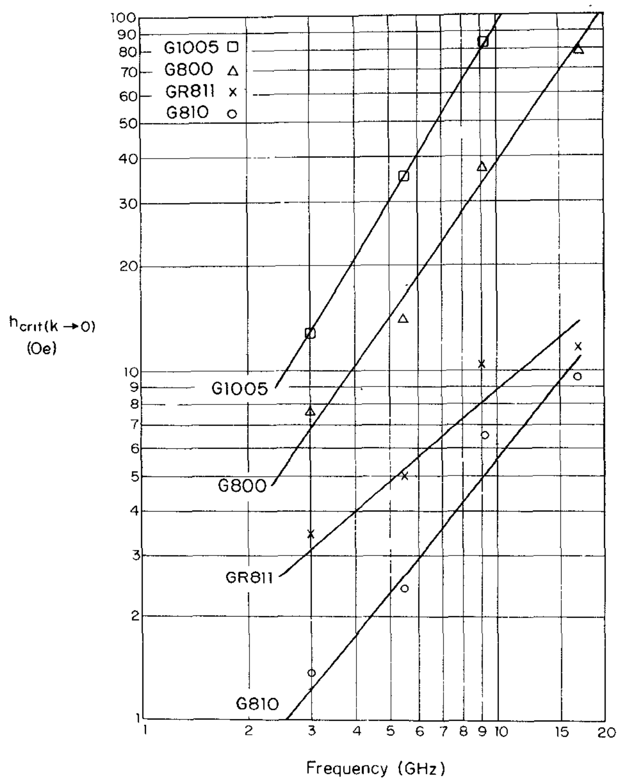

Fig. 9. $h_{crit}(k \rightarrow 0)$ versus frequency for G1005, G800, GR811, and G810.

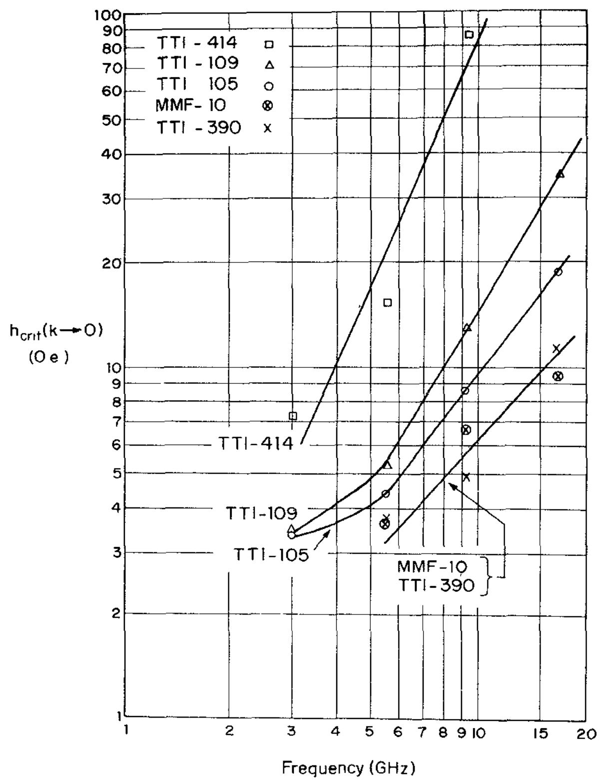

Fig. 11. $h_{crit}(k \rightarrow 0)$ versus frequency for TT1-414, TT1-109, TT1-105, MMF10, and TT1-390.

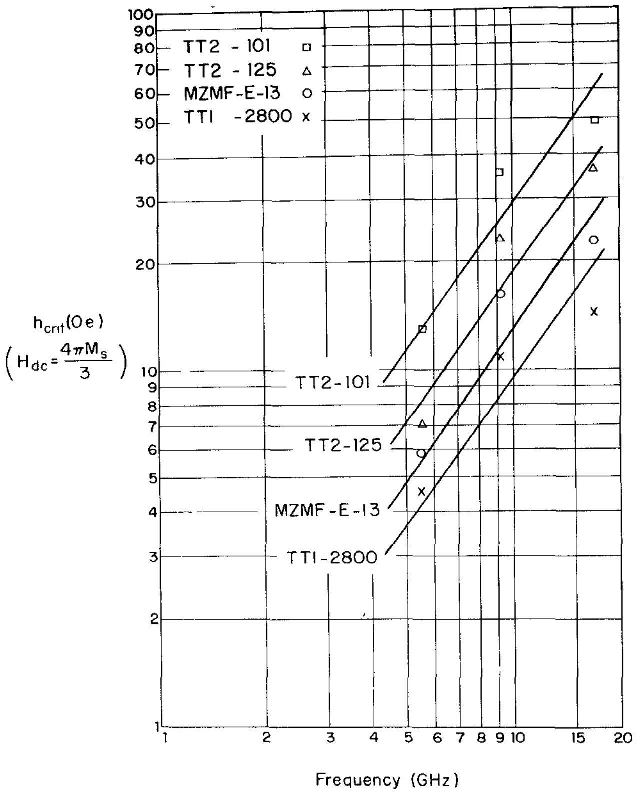

Fig. 12. $h_{crit}(H_{dc} = 4\pi M_s/3)$ versus frequency for TT2-101, TT2-125, MZMF-E-13, and TT1-2800.

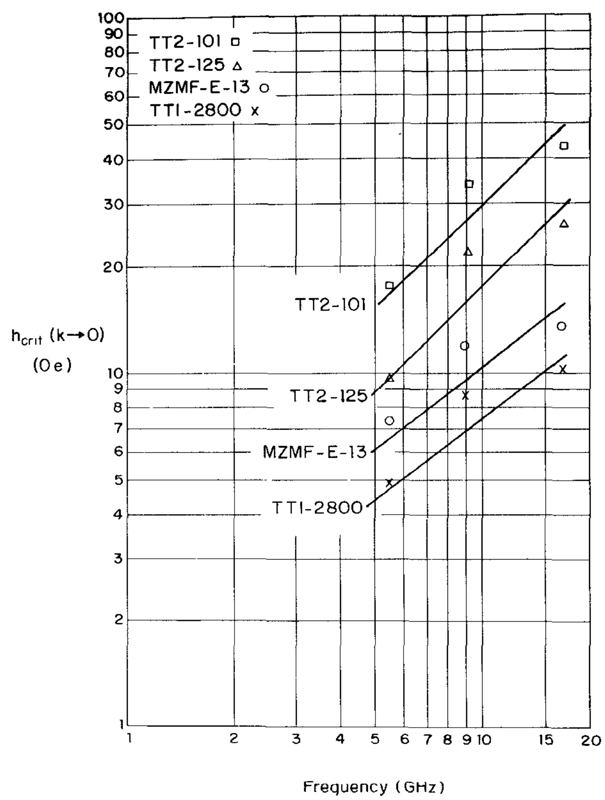

Fig. 13. $h_{crit}(k \rightarrow 0)$ versus frequency for TT2-101, TT2-125, MZMF-E-13, and TT1-2800.

of B and l, ΔH_k was computed from (8) for $\gamma 4\pi M_s/\omega = 0.5$ and is listed in Table I.

From Table I it is evident that a wide range of thresholds are available. Since threshold and loss tend to track each other, it is worth comparing ΔH_{eff} and ΔH_k. The very low loss garnet materials, YIG + Al (G113,G810,G1210) and the YCaVIn garnet (GR1200, GR811, and GR500) have values of ΔH_k which in some cases exceed ΔH_{eff} by a factor of two or more. As gadolinium is added (G1200,G800), both ΔH_{eff} and ΔH_k increase substantially with ΔH_{eff} becoming greater than ΔH_k. For larger gadolinium levels (G1001,G1005) there is further increase in both ΔH_{eff} and ΔH_k with ΔH_{eff} becoming about a factor of 2 greater than ΔH_k. This effect is the result of rare-earth relaxation, and if a further increase in threshold is necessary, either dysprosium or holmium can be added.

The spinels divide into two classes: the magnesium manganese with either aluminum (to lower $4\pi M_s$) or zinc (to raise $4\pi M_s$) and the nickel ferrite with aluminum and cobalt. The magnesium manganese spinels are more lossy than the lowest loss garnets, have values of ΔH_{eff} which are a bit larger than their ΔH_k values, and are similar in this respect to the YIG with Al and Gd. The nickel ferrites are very lossy (note the high ΔH_{eff}) and are rarely used in the partially magnetized applications (e.g., phase shifters or circulators).

V. CONCLUSION

For computer calculations the loss μ_0'' and high power threshold h_{crit} ($H_{dc} = 4\pi M_s/3$) can be characterized by a simple power law in ($\gamma 4\pi M_s/\omega$) [(1) and (7)]. The lowest loss materials are the yttrium aluminum iron garnets. They have the best ratios of threshold to loss with $\Delta H_k/\Delta H_{\text{eff}} > 1$. For the magnesium manganese spinels and the garnets with gadolinium both threshold and loss increase but $\Delta H_k/\Delta H_{\text{eff}} < 1$. The nickel spinels are very lossy.

REFERENCES

[1] C. E. Patton and J. J. Green, "The first-order spin-wave instability threshold in saturated and partially magnetized spheres, rods, and disks of polycrystalline yttrium iron garnet at 9.1 GHz," *IEEE Trans. Magn.*, vol. MAG-5, pp. 626–631, Sept. 1969.

[2] C. E. Patton, "Theory for the first-order spin-wave instability threshold in ferromagnetic insulators of ellipsoidal shape with an arbitrary pumping configuration," *J. Appl. Phys.*, vol. 40, p. 2837, 1969.

[3] J. J. Green, C. E. Patton, and E. Stern, "Threshold microwave field amplitude for the unstable growth of spin waves under oblique pumping," *J. Appl. Phys.*, vol. 40, p. 172, 1969.

[4] J. J. Green, C. E. Patton, and F. Sandy, "Microwave properties of partially magnetized ferrites," Final Rep. RADC-TR-68-312, Aug. 1968.

[5] D. Polder and J. Smit, "Resonance phenomena in ferrites," *Rev. Mod. Phys.*, vol. 25, p. 89, 1953.

[6] C. E. Patton, "Effective linewidth due to porosity and anisotropy in polycrystalline yttrium iron garnet and Ca-V-substituted yttrium iron garnet at 10 GHz," *Phys. Rev.*, vol. 179, p. 352, 1969.

[7] R. I. Joseph and E. Schloemann, "Transient and steady state absorption of microwave power under parallel pumping theory," *J. Appl. Phys.*, vol. 38, p. 1915, 1967.

[8] C. E. Patton, "Effect of grain size on the microwave properties of polycrystalline yttrium iron garnet," *J. Appl. Phys.*, vol. 41, p. 1637, 1970.

[9] J. J. Green and F. Sandy, "Microwave characterization of partially magnetized ferrites, this issue, pp. 641–645.